Supporting Material

Platelet Adhesion from Shear Blood Flow is Controlled by Near-Wall Rebounding Collisions with Erythrocytes

A. A. Tokarev,[†] A. A. Butylin,[†] and F. I. Ataullakhanov[†‡]*

[†]National Research Center for Hematology, Russian Academy of Medical Sciences, Moscow, Russia; [‡]Center for Theoretical Problems of Physicochemical Pharmacology, Russian Academy of Sciences, Moscow, Russia

Address reprint request to F.I. Ataullakhanov, National Research Center for Hematology, Russian Academy of Medical Sciences, Novii Zykovskii proezd, 4a, Moscow, Russia, 125167; tel: +7 495.612.35.22, fax: +7 495.612.88.70, e-mail: fazly@hc.comcor.ru

*Correspondence: fazly@hc.comcor.ru

Table of Contents:

Supplement 1. Estimation of the degree of non-uniformity of the erythrocyte distribution in the perfusion chamber

1.1. Deformation-induced off-wall lateral migration

To evaluate the adequacy of the approximation of uniform erythrocyte distribution under experimental conditions (1-3), we used a simple mathematical model of particle transport in a shear flow, taking into consideration the balance between their shear-induced diffusional and deformation-induced off-wall lateral migration. A similar approach has been successfully applied in earlier studies to describe the non-uniform droplet distribution in diluted and concentrated emulsions in the Couette flow (4,5). Here, it is used to simulate lateral migration of erythrocytes in the in-flow region of the perfusion chamber denoted by light rectangles in Fig. S1, Panel A.

The equation for the balance of erythrocyte volume fraction *Φ(x, y)* had the form

$$\frac{\partial \Phi}{\partial t} + \overline{u}\nabla\Phi = -\nabla\left(-D_{RBC}\nabla\Phi + \overline{V}\Phi\right) \quad \text{(S1).}$$

The erythrocyte dispersion coefficient D_{RBC} was given as the first term of Eq. 4. The velocity of erythrocyte migration from the wall was assumed to be equal to (6,7)

$$\overline{V} \approx k_F \dot{\gamma} \frac{a^3}{h^2}\overline{n} \quad \text{(S2),}$$

where a=2.9 μm is the equivalent radius of a human erythrocyte (radius of the sphere of the same volume), h – distance to the nearest wall, $\overline{n} = \frac{(-v,u)}{|\overline{u}|}$ – normal to the flow velocity $\overline{u} = (u,v)$ directed away from the nearest wall. The value of constant k_F=0.01 was determined in (6) using Eq. S2 for the description of the lateral redistribution of washed human erythrocytes during the passage of their suspension through the constriction in a microfluidic device. To simultaneously account for the opposing walls, the migration velocity $\overline{V}$ was written in the form that additively accounts for them (4,5):

$$\overline{V} = k_F \dot{\gamma} a m \overline{n}, \qquad \text{where } m = \frac{a^2}{h_{bottom}^2} - \frac{a^2}{h_{top}^2} \quad \text{(S3).}$$

Here, h_{bottom} and h_{top} are the distances to the lower (i.e., on the right of the flow direction) and the upper (i.e., on the left of the flow direction) walls, respectively. Because at shear rates above ~50 s^{-1} the viscosity of blood and RBC suspension shows only weak dependence on the shear rate (8) and the near-wall erythrocyte distribution was of primary interest, the velocity field was found by solving the Navier-Stokes equations with constant viscosity (9):

$$\rho\frac{\partial \overline{u}}{\partial t} + \rho(\overline{u}\nabla)\overline{u} = \nabla\left(-pI + \eta\left(\nabla\overline{u} + (\nabla\overline{u})^T\right)\right), \quad \nabla\cdot\overline{u} = 0 \quad \text{(S4).}$$

Here, ρ and μ are mean density and viscosity of blood, p – pressure, I – unit tensor. The local shear rate was determined as (9)

$$\dot{\gamma} = \left(2u_x^2 + (u_y + v_x)^2 + 2v_y^2\right)^{1/2} \quad \text{(S5),}$$

where subscripts x and y denote the respective spatial derivatives.

Equations S1 and S4 were made dimensionless as follows: $x' = x/H$, $y' = y/H$, $t' = t\dot{\gamma}_w$, $u' = u/u_0$, $v' = v/u_0$, $p' = p/p_0$, $\dot{\gamma}' = \dot{\gamma}/\dot{\gamma}_w$, $a' = a/H$, $h'_{bottom} = h_{bottom}/H$, $h'_{top} = h_{top}/H$, where $u_0 = H\dot{\gamma}_w$, $p_0 = \eta\dot{\gamma}_w$, H=600 μm. After that, they assumed the form (hereafter, the primes are omitted):

$$\frac{\partial \Phi}{\partial t} + \overline{u}\nabla\Phi = -a^2\nabla\left[\dot{\gamma}\left(-k_{ZC}\Phi(1-\Phi)^{0.8}\nabla\Phi + \frac{k_F}{a}m\overline{n}\Phi\right)\right] \quad \text{(S6),}$$

$$\frac{\partial \overline{u}}{\partial t} + (\overline{u}\nabla)\overline{u} = \frac{1}{\mathrm{Re}}\nabla\left(-pI + \nabla\overline{u} + (\nabla\overline{u})^T\right), \quad \nabla\cdot\overline{u} = 0 \qquad \text{(S7)},$$

where $\mathrm{Re} = \dot{\gamma}_w H^2 \frac{\rho}{\eta}$ is the Reynolds number. The form of expressions for m and $\dot{\gamma}$ did not change after they were made dimensionless (Eqs. S3 and S5). The coordinates were normalized to H, the dimensionless width of the channel in the region farthest from the inlet was 2, the entrance width was 5, and the total length of the computational region was 10.8 (see the bottom part of the Panel B in Fig. S1). In order to have the dimensionless wall shear rate equal to 1, the entrance velocity profile was parabolic with the maximum 0.5×2/5=0.2. The inflow erythrocyte distribution was assumed to be uniform and correspond to $\Phi_{RBC,0}$=0.4. To avoid a singularity in the calculation of m, the distances h_{bottom} and h_{top} in Eq. S3 were increased by a small value, a/4; this addition is much smaller than the erythrocyte diameter and therefore does not significantly affect the result.

Equations S6 and S7 were solved in the steady-state case. At first, the velocity field was found by solving the Eq. S7, and then the distribution of the erythrocyte volume fraction was found by solving the Equation S6. Panel B in Fig. S1 shows the distribution of velocities (arrows) and erythrocyte volume fraction (surface) at the characteristic wall shear rate in the experiments being simulated ($\dot{\gamma}_w$=800 s^{-1}). In general, erythrocytes are distributed uniformly even though the layer near both walls is somewhat depleted. The depletion is established rapidly at the entrance of both the wide and the narrow zones and does not vary further downstream (a small bend near the outflow boundary x=5 is a numerical artifact). Panel C shows the distribution of the erythrocyte volume fraction across the flow at x = 3 (equivalent to 1800 μm from the wall curve). Evidently, the erythrocyte-depleted region is roughly 10 μm thick, i.e., comparable with the main diameter of a human erythrocyte. The mean value of Φ_{RBC} over a section of 0…8 μm is around 0.34, which is 15% lower than $\Phi_{RBC,0.}$ Therefore, the non-uniform distribution of erythrocytes resulting from their deformation-induced off-wall migration can be neglected under these conditions.

1.2. Shear diffusion-induced lateral migration

Another mechanism for formation of the non-uniform particle distribution across the flow is lateral migration resulting from particle-particle collisions (see reviews in(10-12)). It is a consequence of collision irreversibility and does not depend on particle interactions with the fluid and the wall. The transition length along the chamber necessary to form a non-uniform distribution of erythrocytes by this mechanism was estimated using the formula from(10):

$$L_{ss} = \frac{H}{12 D_{RBC}(\Phi)/\dot{\gamma}a^2}\left(\frac{H}{a}\right)^2 \qquad \text{(S8)}.$$

Taking D_{RBC} as the first term of Equation 4 and substituting $d_{RBC}/2$ with a yields

$$L_{ss} = \frac{H}{12 k_{ZC}\Phi_{RBC}\left(1-\Phi_{RBC}\right)^{0.8}}\left(\frac{H}{a}\right)^2 \qquad \text{(S9)}.$$

Thus, the calculated L_{ss} for human or rabbit RBSs at 40% hematocrit equals ~$5\cdot10^7$ μm = 50 m, which is substantially greater not only than the inflow chamber length but also than its whole length. Thus, the lateral migration resulting from this mechanism was nonessential in the experiments being considered.

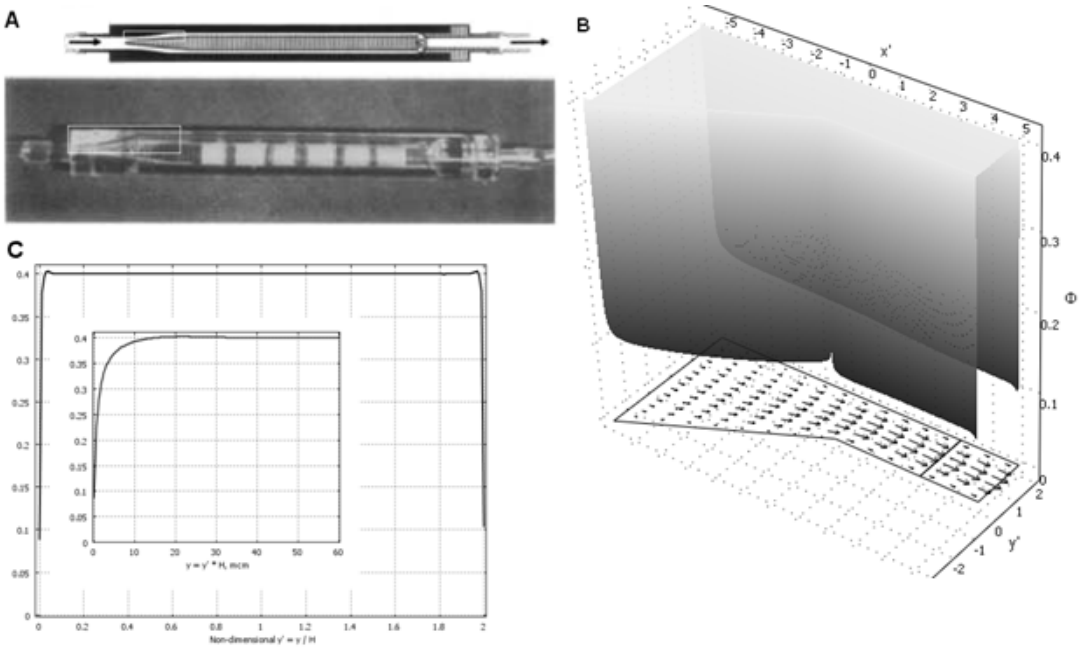

Figure S1. Erythrocyte distribution in the perfusion chamber. (A) A general view of the chamber from(13): schematic (top) and photograph (bottom). The arrows indicate the blood flow direction. The photograph shows arterial segments exposed to the blood. The region of subsequent calculation of erythrocyte distribution is marked by light rectangles. (B) The calculated steady-state velocity field (*arrows*) and the erythrocyte volume fraction distribution (*surface*) over the inflow chamber region at $\dot{\gamma}_w$=800 s^{-1} (corresponding to *Re*=64 because the mean kinematic viscosity of blood is $\eta/\rho = 4.5\times10^6\ \mu m^2/s$). The narrow layer near both walls is depleted of erythrocytes. The cross-section at *x*=3, i.e., 1800 μm from the wall curve, is shown as a black segment. (C) The distribution of the erythrocyte volume fraction within the cross section at *x*=3, 0≤*y*≤2. The inset shows the detailed view of the segment near *y=0*, indicating that the thickness of the depleted zone is roughly equal to the main erythrocyte diameter.

Supplement 2. Platelet flux to the wall

The expression for platelet flux to the wall (the number of platelet-wall collisions per unit area per unit time) was derived using the assumption that the only platelets to interact with the wall are those that were expelled toward it from the narrow near-wall layer as a result of inelastic rebounding collision with another blood cell (either erythrocyte or another platelet) that travels slightly further from the wall and therefore with a higher velocity (Fig. 1A). The flux J was determined by the product of collision frequency of a single platelet, ν, platelet two-dimensional concentration in the near-wall layer, S (platelets/μm^2), and hydrodynamic collision efficiency, ε_h. Neglecting hydrodynamic interactions between the particles as well as between the particles and the wall, Smoluchowski's theory gives the following expression for the collision frequency of two spheres of volume V_1 and V_2 approaching each other by rectilinear paths in a simple shear flow (14-16):

$$\beta = \frac{\dot{\gamma}}{\pi}\left(V_1^{1/3} + V_2^{1/3}\right)^3 \quad \text{(S10)},$$

where $\dot{\gamma}$ is the local shear rate. After expressing the sphere volume through its radius, substituting it by the major radius of an erythrocyte, $d_{RBC}/2$ or platelet, $d_P/2$, corrected with factors k_1 and k_2, it became

$$\beta_1 = \frac{4}{3}\dot{\gamma}\left(k_1\frac{d_P}{2} + k_2\frac{d_{\mathrm{RBC}}}{2}\right)^3 \quad \text{(S11)},$$

The introduction of factors k_1 and k_2 was required due to the non-spherical shape of blood cells and presence of the wall, which may influence their interactions in a shear flow (17). This influence is insufficiently investigated, thus k_1- and k_2-values should be determined from the comparison of theoretical predictions with experimental data (see Fig. 4A).

The frequency of collisions of a single platelet with erythrocytes near the wall was estimated as

$$\begin{aligned}\nu_1 &\approx \frac{1}{2}\beta_1 n_{\mathrm{RBC}} = \frac{1}{2}\frac{4}{3}\dot{\gamma}_w\left(k_1\frac{d_P}{2} + k_2\frac{d_{\mathrm{RBC}}}{2}\right)^3 n_{\mathrm{RBC}} = \\ &= \frac{\left(k_1 d_P + k_2 d_{\mathrm{RBC}}\right)^3}{12V_{RBC}}\dot{\gamma}_w\Phi_{\mathrm{RBC}} = K_1\left(d_P, d_{\mathrm{RBC}}, V_{\mathrm{RBC}}\right)\dot{\gamma}_w\Phi_{\mathrm{RBC}}\end{aligned} \quad \text{(S12)},$$

where $\dot{\gamma}_w$ is the wall shear rate, n_{RBC} and Φ_{RBC} are the erythrocyte concentration and volume fraction, respectively, V_{RBC} is the volume of an erythrocyte, and $K_1\left(d_P, d_{\mathrm{RBC}}, V_{\mathrm{RBC}}\right) = \frac{\left(k_1 d_P + k_2 d_{\mathrm{RBC}}\right)^3}{12V_{RBC}}$. Factor ½ in Eq. S12 takes into account the absence of erythrocytes between the wall and the platelet flowing close to it. By analogy, the frequency of collisions of a single platelet with other platelets was

$$\nu_2 \approx \frac{1}{2}\frac{4}{3}\dot{\gamma}_w\left(k_1\frac{d_P}{2} + k_2\frac{d_P}{2}\right)^3 P = \frac{\left(k_1 + k_2\right)^3 d_P^3}{12V_P}\dot{\gamma}_w V_P P = K_2\left(d_P, V_{\mathrm{P}}\right)\dot{\gamma}_w V_P P \quad \text{(S13)},$$

where $K_2\left(d_P, V_{\mathrm{P}}\right) = \frac{\left(k_1 + k_2\right)^3 d_P^3}{12V_P}$, and V_p is the platelet volume. For simplicity, the "shape factors" k_1 and k_2 were assumed to be identical in Eqs. S12 and S13.

The lateral displacement of particles resulting from one inelastic rebounding collision in a viscous media is of the order of particle's dimension (10,18). Thus, the thickness of the layer from which a platelet can be expelled by an erythrocyte or another platelet toward the wall in the result of one collision was roughly estimated as d_{RBC} and d_P, respectively. Platelet two-dimensional concentration in these layers is $S_1 = P \times d_{RBC}$ and $S_2 = P \times d_P$.

Actual collision frequency of particles in an unbounded shear flow is lower then one predicted by Smoluchowski's theory (Eq. S10) due to their hydrodynamic interaction. The measure of this inequality calls the hydrodynamic collision efficiency. Earlier studies have demonstrated that hydrodynamic collision efficiency for spheres (19) and platelets and their aggregates (14), which were assumed to be spherical, depends on both the shear rate and the size ratio of colliding particles λ. For $0.3 \le \lambda \le 1$, this dependency was expressed in the form (14)

$$\varepsilon_h(\lambda,\dot{\gamma}) = X_1(\lambda)\left(\frac{2.725}{\dot{\gamma}}\right)^{Y_1(\lambda)} \quad \text{(S14)},$$

where

$$\begin{aligned} X_1(\lambda) &= -0.2258\lambda^3 - 0.1579\lambda^2 + 0.7356\lambda + 0.1077 \\ Y_1(\lambda) &= -1.1866\lambda^3 + 2.7509\lambda^2 - 2.0556\lambda + 0.6411 \end{aligned} \quad \text{(S15)}.$$

Assuming that Eq. S14 is applicable for platelet-erythrocyte ($\lambda_1 = \frac{d_P}{d_{RBC}}$, $\varepsilon_1 = \varepsilon_h\left(\frac{d_P}{d_{RBC}}, \dot{\gamma}_w\right)$) and platelet-platelet ($\lambda_2 = 1$, $\varepsilon_2 = \varepsilon_h(1, \dot{\gamma}_w)$) collisions near the wall, platelet fluxes to the wall generated by these collisions were calculated as the following expressions:

$$\begin{aligned} J_1 &= \varepsilon_1 \nu_1 S_1 = \varepsilon_1 K_1 d_{RBC} \dot{\gamma}_w \Phi_{\mathrm{RBC}} P \\ J_2 &= \varepsilon_2 \nu_2 S_2 = \varepsilon_2 K_2 d_P \dot{\gamma}_w V_{\mathrm{P}} P^2 \end{aligned} \quad \text{(S16)}.$$

The total platelet flux toward the wall was their sum:

$$J = J_1 + J_2 = \left(\varepsilon_1 K_1 d_{RBC} \Phi_{\mathrm{RBC}} + \varepsilon_2 K_2 d_P V_{\mathrm{P}} P\right)\dot{\gamma}_w P = Q\dot{\gamma}_w P \quad \text{(S17)}.$$

The characteristic sizes of platelets and erythrocytes along with the values of $\varepsilon_{1,2}$ calculated at the necessary shear rates are shown in Tables S1 and S2.

Tables

Table S1. The mean size of rabbit erythrocytes and platelets and the typical efficiency of their hydrodynamic interaction

	Rabbit RBC	Rabbit platelet
d, μm	6[*)]	2[†)]
V, μm^3	70[*)]	2.4[‡)]
λ	λ_1=0.333	λ_2=1
$X_1(\lambda)$	0.327	0.460
$Y_1(\lambda)$	0.218	0.150
$\varepsilon_h\left(\lambda, \dot{\gamma}_w = 832 s^{-1}\right)$	ε_1=0.0942	ε_2=0.195

*) See reference (3)

†) See reference (1)

‡) Estimated from the size of human platelets (Table 2) as $V_{P,rabbit} = V_{P,human} \times \left(d_{P,rabbit} / d_{P,human}\right)^3$

Table S2. The mean size of human, rabbit and goat erythrocytes and human platelets and the typical efficiency of their hydrodynamic interaction

	Human RBC	Rabbit RBC	Goat RBC	Human platelet
d, μm	8[*)]	6[*)]	3[*)]	3[†)]
V, μm^3	95[*)]	70[*)]	25[*)]	8[†)]
λ	λ_1=0.375	λ_1=0.5	λ_1=1	λ_2=1
$X_1(\lambda)$	0.349	0.408	0.460	0.460
$Y_1(\lambda)$	0.195	0.153	0.150	0.150
$\varepsilon_h\left(\lambda, \dot{\gamma}_w = 800 s^{-1}\right)$	ε_1=0.116	ε_1=0.171	ε_1=0.196	ε_2=0.196

*) See reference (3)

†) See reference (20)

REFERENCES

1. Turitto, V. T. and H. R. Baumgartner. 1975. Platelet deposition on subendothelium exposed to flowing blood: mathematical analysis of physical parameters. *Trans. Am. Soc. Artif. Intern. Organs* 21:593-601.

2. Turitto, V. T. and H. R. Baumgartner. 1979. Platelet interaction with subendothelium in flowing rabbit blood: effect of blood shear rate. *Microvasc. Res.* 17:38-54.

3. Aarts, P. A., P. A. Bolhuis, K. S. Sakariassen, R. M. Heethaar, and J. J. Sixma. 1983. Red blood cell size is important for adherence of blood platelets to artery subendothelium. *Blood* 62:214-217.

4. Hudson, S. D. 2003. Wall migration and shear-induced diffusion of fluid droplets in emulsions. *Physics of Fluids* 15:1106-1113.

5. King, M. R. and D. T. Leighton, Jr. 2001. Measurement of shear-induced dispersion in a dilute emulsion. *Physics of Fluids* 13:397-406.

6. Faivre, M., M. Abkarian, K. Bickraj, and H. A. Stone. 2006. Geometrical focusing of cells in a microfluidic device: An approach to separate blood plasma. *Biorheology* 43:147-159.

7. Olla, P. 1997. The lift on a tank-treading ellipsoidal cell in a shear flow. *Journal de Physique II* 7:1533-1540.

8. Goldsmith, H. L. and V. T. Turitto. 1986. Rheological aspects of thrombosis and haemostasis: basic principles and applications. ICTH-Report--Subcommittee on Rheology of the International Committee on Thrombosis and Haemostasis. *Thromb. Haemost.* 55:415-435.

9. Quarteroni, A. M., M. Tuveri, and A. Veneziani. 2000. Computational vascular fluid dynamics: problems, models and methods. *Computing and Visualization in Science* 2:163-197.

10. Nott, P. R. and J. F. Brady. 1994. Pressure-driven flow of suspensions: simulation and theory. *Journal of Fluid Mechanics* 275:157-199.

11. Koh, C. J., P. Hookham, and L. G. Leal. 1994. An experimental investigation of concentrated suspension flows in a rectangular channel. *Journal of Fluid Mechanics* 266:1-32.

12. Lyon, M. K. and L. G. Leal. 1998. An experimental study of the motion of concentrated suspensions in two-dimensional channel flow. Part 1. Monodisperse systems. *Journal of Fluid Mechanics* 363:25-56.

13. Baumgartner, H. R. 1973. The role of blood flow in platelet adhesion, fibrin deposition, and formation of mural thrombi. *Microvasc. Res.* 5:167-179.

14. Tandon, P. and S. L. Diamond. 1997. Hydrodynamic effects and receptor interactions of platelets and their aggregates in linear shear flow. *Biophys. J.* 73:2819-2835.

15. Bonnefoy, A., Q. Liu, C. Legrand, and M. M. Frojmovic. 2000. Efficiency of platelet adhesion to fibrinogen depends on both cell activation and flow. *Biophys. J.* 78:2834-2843.

16. Huang, P. Y. and J. D. Hellums. 1993. Aggregation and disaggregation kinetics of human blood platelets: Part I. Development and validation of a population balance method. *Biophys. J.* 65:334-343.

17. Mody, N. A. and M. R. King. 2008. Platelet adhesive dynamics. Part I: characterization of platelet hydrodynamic collisions and wall effects. *Biophys. J.* 95:2539-2555.

18. Phillips, R. J., R. C. Armstrong, and R. A. Brown. 1992. A constitutive equation for concentrated suspensions that accounts for shear-induced particle migration. *Phys. Fluids A* 4:30-40.

19. van de Ven, T. and S. G. Mason. 1977. The microrheology of colloidal dispersions VII. Orthokinetic doublet formation of spheres. *Colloid & Polymer Sci.* 255:468-479.

20. Goldsmith, H. L. and R. Skalak. 1975. Hemodynamics. *Annual Review of Fluid Mechanics* 7:213-247.